IEEE Access
Multidisciplinary | Rapid Review | Open Access Journal

Received June 11, 2019, accepted July 14, 2019, date of publication July 17, 2019, date of current version August 6, 2019.

Digital Object Identifier 10.1109/ACCESS.2019.2929549

Performance Analysis of Directional Modulation With Finite-Quantized RF Phase Shifters in Analog Beamforming Structure

JIAYU LI[1], LING XU[1], PING LU[2], TINGTING LIU[3], (Member, IEEE), ZHIHONG ZHUANG[1], JINSONG HU[4], FENG SHU[1], (Member, IEEE), AND JIANGZHOU WANG[5], (Fellow, IEEE)

[1]School of Electronic and Optical Engineering, Nanjing University of Science and Technology, Nanjing 210094, China
[2]Zhongxing Telecommunication Equipment Corporation, ShenZheng 518057, China
[3]School of information and communication engineering, Nanjing Institute of Technology, Nanjing 211167, China
[4]College of Physics and Information, Fuzhou University, Fuzhou 350116, China
[5]School of Engineering and Digital Arts, University of Kent, Canterbury CT2 7NT, U.K.

Corresponding author: Jinsong Hu (jinsong.hu@fzu.edu.cn)

This work was supported in part by the National Natural Science Foundation of China under Grant 61771244, Grant 61472190, Grant 61501238, and Grant 61702258.

ABSTRACT The radio frequency (RF) phase shifter with finite quantization bits in analog beamforming (AB) structure forms quantization error (QE) and causes a performance loss of received signal to interference plus noise ratio (SINR) at the receiver (called Bob). By using the law of large numbers in probability theory, the closed-form expression of the SINR performance loss is derived to be inversely proportional to the square of Sinc (or $\sin(x)/x$) function. Here, a phase alignment method is applied in the directional modulation transmitter with the AB structure. Also, the secrecy rate (SR) expression is derived with the QE. From the numerical simulation results, we find that the SINR performance loss gradually decreases as the number L of quantization bits increases. This loss is less than 0.3 dB when L is larger than or equal to three. As L exceeds five, the SINR performance loss at Bob can be approximately trivial. Similarly, the SR performance loss gradually reduces as L increases. In particular, the SR performance loss is about 0.1 bits/s/Hz for L=3 at signal-to-noise ratio of 15 dB.

INDEX TERMS Directional modulation, quantization error, quantized phase shifter, analog beamforming.

I. INTRODUCTION

Directional modulation (DM), as one of the key technologies of wireless physical layer security, is attracting ever-increasing research interests and activities from both academia and industry world. Traditional technology for directional modulation was proposed on the radio frequency (RF) frontend [1]–[3]. In these articles, the authors proposed an actively driven DM array of utilizing analog RF phase shifters or antenna elements, which did not deal with the flexibility of design process. Another way to implement the DM synthesis is based on the baseband signal processing. In [4], the authors proposed to form an orthogonal vector, which can be updated in the null space of channel vector at the desired direction, to the transmitted baseband signal as artificial noise (AN), thereby improving the secure transmission. Compared to the design on the RF frontend, this approach enables dynamic DM transmissions and makes the design easier. Realizing directional modulation in practice is not a trivial task. One key point is how to use AN against the overhearing of the potential eavesdroppers. In [5], the authors thoroughly studied the secrecy performance of three AN-aided secure transmission schemes and examined the possibility and strategy of using the full-duplex receiver to transmit AN in covert communications [6], [7]. Furthermore, a practical DM scheme with random frequency diverse array with the aid of AN is proposed to enhance physical layer security for the wireless communications system [8].

In the presence of direction measurement error, the authors in [9], [10] and [11] proposed three robust DM synthesis methods for three different scenarios: single-desired user, multi-user broadcasting and multi-user multi-input

The associate editor coordinating the review of this manuscript and approving it for publication was Ke Guan.

multi-output (MIMO) by fully exploiting the statistical properties of direction measurement error. Reference [12] proposed two secure schemes, Max-GRP plus NSP and Max-SLNR plus Max-ANLNR, for multicast DM scenario to improve the security. Inspired by the work in [13] and [14], secure and precise wireless transmission (SPWT) proposed in [15] combined AN projection, beamforming and random subcarrier selection based on orthogonal frequency division multiplexing (OFDM) to achieve SPWT of confidential messages. In the researches mentioned above, the DM synthesis on the baseband signal processing is assumed perfect or imperfect channel state information (CSI). In [16], the authors proposed three estimators of directions of arrival (DOA) based on hybrid structure for finding direction, thereby determining the position. This method makes DM more practical.

In [9], [10], and [11], the authors proposed robust methods for imperfect CSI in traditional DM systems, i.e, fully-digital (FD) beamforming systems. Traditional fully-digital beamforming technique is of high cost and power consumption due to each antenna element requiring one dedicated RF chain. Hybrid analog/digital (HAD) beamforming structure [17]–[19] with analog phase shifters and a reduced number of RF chains was proposed to strike a good balance between the system complexity and the beamforming precision. Compared to HAD and FD beamforming structures, analog beamforming (AB) structure with digitally-controlled phase shifters has attracted substantial research attentions from both industry and academic communities, due to its low circuit cost and high energy efficiency [20]–[23]. In general, AB structure has only single RF chain linked to all antennas. However, AB as described in [21], [23] is subject to additional constraints, for example, the digitally-controlled phase shifters with finite-quantized phase values and constant-envelope. Here, due to finite-quantized phase values, there exists quantization error (QE), which will lead to a performance loss such as signal to interference plus noise ratio (SINR) and secrecy rate (SR). It is crucial to derive and analyze the impact of QE on SINR and SR due to the accuracy of quantization of phase shifter. To achieve an allowable performance loss, what is the minimum number of quantization bits compared with infinite-bit quantization (no QE, NQE)? In what follows, we will address this issue.

In this paper, we will mainly present analysis of the effect of QE from finite-quantized phase shifters on the performance of DM system using AB structure. Here, the transmitter Alice is equipped with an AB structure, while the desired receiver at Bob works in full-duplex model and helps Alice by transmitting AN with FD beamforming structure to degrade the performance of the illegitimate receiver at Eve. The main contributions of this paper are summarized as follows:

1) In AB structure, the RF phase shifter with finite quantization bits will lead to degradation of the value of the received SINR at Bob. By using the law of large numbers in probability theory, the approximate closed-form expression of SINR performance loss is derived to be inversely proportional to the square of sinc (i.e., $\sin(x)/x$) function. Simulation results indicate that the SINR performance loss is less than 0.3 dB when the number L of quantization bits is no less than 3. As the number of quantization bits is larger than 4, the SINR performance loss at Bob can be completely negligible. This will greatly simplify the analysis that how many bits are sufficient such that the loss of SINR can be omitted in the AB structure.
2) In the presence of QE, the expression of SR is also derived and simplified. Simulation results indicate that the SR performance loss is about 0.1 bits/s/Hz when $L = 3$. More importantly, as the value of L increases, the SR performance loss decreases gradually. Thus, $L = 3$ is sufficient for RF phase quantizer in the AB structure.

The remainder of this paper is organized as follows. Section II describes the system model. In Section III, the expression of SINR loss is derived by modeling quantization error as a uniform distribution, and at the same time the corresponding SR expression is given in the presence of QE. Simulation results are presented in Section IV. Finally, we make our conclusions in Section V.

Notations: throughout the paper, matrices, vectors, and scalars are denoted by letters of bold upper case, bold lower case, and lower case, respectively. Signs $(\cdot)^T$, $(\cdot)^*$, $(\cdot)^H$ and $|\cdot|$ denote transpose, conjugate, conjugate transpose and modulus respectively. Notation $\mathbb{E}\{\cdot\}$ stands for the expectation operation.

II. SYSTEM MODEL

Consider a DM network with a Gaussian wiretap channel in Fig. 1, where Alice is equipped with N_a antennas, Bob is equipped with N_b antennas, and Eve is equipped with single antenna. Alice intends to send its confidential message x to Bob, without being wiretapped by Eve. The DM transmitter at Alice adopts an AB structure. This means Alice can send single confidential message stream to Bob by analog beamforming due to only one RF chain. In order to help Alice, Bob operates in a FD mode. In other words, all antennas at Bob are partitioned into two subsets. The first subset with N_b^t antennas transmits AN z, and the rest part with $N_b^r = N_b - N_b^t$ antennas receive the confidential messages from Alice. For the case $N_b^r = 1$, Bob only employ one single antenna to receive the signal as Eve do, which can be achieved by the selection combing scheme [24]. The multiple-input-single-output (MISO) model in physical layer security system usually can be regarded as a start point to examine the secure transmission [7], [25]. In the future work, we will focus on scenarios where the number of antennas at eavesdropper Eve is larger than 1 and provide more detailed results relating to it. Since Bob transmits AN while receiving the desired

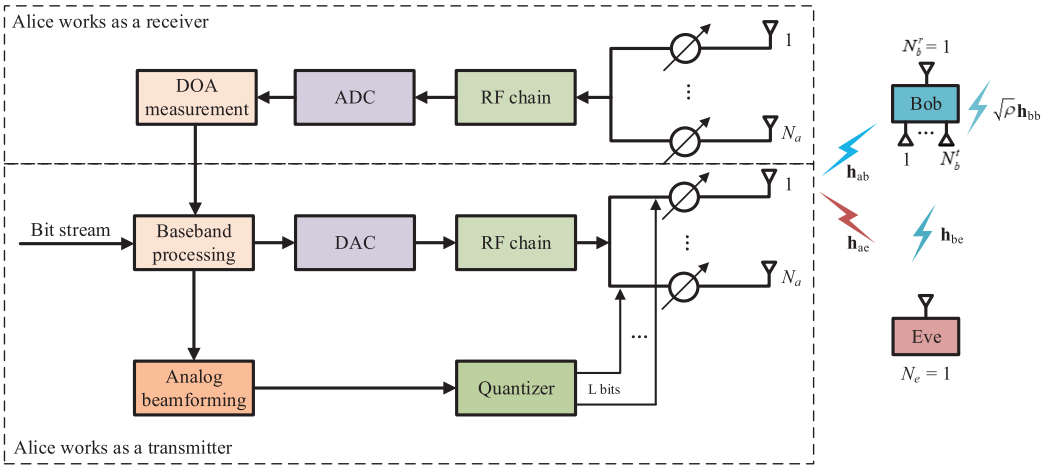

FIGURE 1. System model.

signal, there always exists self-interference at its own receive signal. To describe the effect of residual self-interference we employ the loop interference model of [26], which quantifies the level of self-interference with a parameter $\rho \in [0, 1]$, with $\rho = 0$ denoting zero self-interference. In this paper, we assume there exists the line-of-sight (LOS) path. The transmit signal at Alice and AN at Bob can be respectively written as

$$\mathbf{s}_a = \sqrt{P_a}\mathbf{v}_a x, \tag{1}$$

and

$$\mathbf{s}_b = \sqrt{P_b}\mathbf{v}_b z, \tag{2}$$

where P_a and P_b are the transmission powers of Alice and Bob, respectively. Vector

$$\mathbf{v}_a(\alpha) = \frac{1}{\sqrt{N_a}}\left[e^{j\hat{\alpha}_1}, e^{j\hat{\alpha}_2}, \cdots, e^{j\hat{\alpha}_{N_a}}\right]^T \tag{3}$$

denotes the transmit analog beamforming vector, which forces the confidential message to the desired direction and $\mathbf{v}_b \in \mathbb{C}^{N_b \times 1}$ is the beamforming vector of transmitting AN to interfere with Eve. An AB pattern is generated by a digitally-controlled RF phase-shifter with L-bit phase quantizer. This means that each antenna's phase in (3) takes one nearest value $\hat{\alpha}_n$ to the designed value α_n from a set of 2^L quantized phases given by

$$\hat{\alpha}_n \in \Theta = \left\{0, 2\pi(\frac{1}{2^L}), 2\pi(\frac{2}{2^L}), \cdots, 2\pi(\frac{2^L-1}{2^L})\right\}, \tag{4}$$

which is actually an integer optimization problem. Therefore, the beamforming vector in the AB system is defined with the quantized phases α_n and written as (3). Each element phase is quantized to L bits. In (1), x is the confidential message of satisfying $\mathbb{E}\{x^H x\} = 1$. We assume that the AN z transmitted by Bob obeys a Gaussian distribution with zero mean and $\mathbb{E}\{z^H z\} = 1$.

Taking the path loss into consideration, the signal received at Bob and Eve can be respectively written as

$$\begin{aligned} y_b &= \sqrt{g_{ab}}\mathbf{h}_{ab}^H(\theta_d)\mathbf{s}_a + \sqrt{\rho}\mathbf{h}_{bb}^H\mathbf{s}_b + n_b \\ &= \sqrt{g_{ab}P_a}\mathbf{h}_{ab}^H(\theta_d)\mathbf{v}_a x + \sqrt{\rho P_b}\mathbf{h}_{bb}^H\mathbf{v}_b z + n_b, \end{aligned} \tag{5}$$

and

$$\begin{aligned} y_e &= \sqrt{g_{ae}}\mathbf{h}_{ae}^H(\theta_e)\mathbf{s}_a + \sqrt{g_{be}}\mathbf{h}_{be}^H\mathbf{s}_b + n_e \\ &= \sqrt{g_{ae}P_a}\mathbf{h}_{ae}^H(\theta_e)\mathbf{v}_a x + \sqrt{g_{be}P_b}\mathbf{h}_{be}^H\mathbf{v}_b z + n_e, \end{aligned} \tag{6}$$

where $g_{ab} = \frac{\epsilon}{d_{ab}^c}$ and d_{ab} denote the loss coefficient and distance between Alice and Bob respectively. c is the path loss exponent and ϵ is the attenuation at reference distance d_0. Likewise, $g_{ae} = \frac{\epsilon}{d_{ae}^c}$ and d_{ae} denote the loss coefficient and distance between Alice and Eve, respectively. $g_{be} = \frac{\epsilon}{d_{be}^c}$ and d_{be} denote the loss coefficient and distance between Bob and Eve, respectively. $n_b \sim \mathcal{CN}(0, \sigma_b^2)$ and $n_e \sim \mathcal{CN}(0, \sigma_e^2)$ represent complex additive white Gaussian noise (AWGN) at Bob and Eve, respectively. $\mathbf{h}_{ab} \in \mathbb{C}^{N_a \times 1}$ denotes the channel vector from Alice to Bob, $\mathbf{h}_{ae} \in \mathbb{C}^{N_a \times 1}$ and $\mathbf{h}_{be} \in \mathbb{C}^{N_b^t \times 1}$ denote the channel vectors from Alice and Bob to Eve, respectively. $\mathbf{h}_{bb} \in \mathbb{C}^{N_b^t \times 1}$ represents the self-interference channel vector at Bob. In the following, we assume that $\sigma_b^2 = \sigma_e^2 = \sigma^2$.

In Fig. 1, the transmitter is deployed with an N_a-element linear antenna array. The normalized steering vector (NSV) for the transmit antenna array is denoted by

$$\mathbf{h}(\theta) = \left[e^{j2\pi\Psi_\theta(1)}, \cdots, e^{j2\pi\Psi_\theta(n)}, \cdots, e^{j2\pi\Psi_\theta(N_a)}\right]^T, \tag{7}$$

and the phase function $\Psi_\theta(n)$ is defined as

$$\Psi_\theta(n) \triangleq -\frac{(n-(N_a+1)/2)d\cos\theta}{\lambda}, \quad n = 1, 2, \cdots, N_a, \tag{8}$$

where θ is the direction angle, n denotes the n-th antenna, d is the distance of two adjacent antennas, and λ is

the wavelength. Making use of the definition of NSV, we have $\mathbf{h}_{ab}(\theta_d) = \mathbf{h}(\theta_d)$ and $\mathbf{h}_{ae}(\theta_e) = \mathbf{h}(\theta_e)$. The potential eavesdroppers may be passive and never transmit signals, thus means it is hard to obtain such location information. Considering a realistic scenario, the location of Eve may exist at an annular region centered on the location of Bob, which is similar to the annulus threat model mentioned in [27].

If the beamforming vector $\mathbf{v}_a$ is determined, the optimal $\mathbf{v}_b$ can be solved by using the Max-SR method [28] and utilizing the GPI algorithm [29]. Suppose that the total duration of each block consists of pilot symbol periods and data symbol periods separately. During the pilot symbol periods, Alice and Bob send pilots to enable the estimation of the main channel and the self-interference channel. In the data symbol periods, Alice transmits confidential information to Bob, while the full-duplex Bob sends artificial noise to aid the secure transmission. According to the method mentioned in [30], the optimal value of P_b can be obtained by maximizing the probability of achieving reliable decoding as for Bob under the predetermined secrecy requirement of the system.

III. DERIVATION OF SINR AND SR PERFORMANCE LOSS EXPRESSIONS

In this paper, we focus on the impact of quantization error of the phase shifter on SINR and SR performance, which will cause phase mismatch between the NSV $\mathbf{h}$ and the AB vector even with ideal measurement of direction. This will degrade the receive performance at Bob, including the receive SINR loss and SR reduction. The small QE in the phase shifter may severely degrade the performance of the DM system. The desired direction angle from Alice and Bob is denoted by θ_d. In practice, the angle θ_d is not a certain value, but will be offset around a value that can be estimated by the high-resolution and low-complexity ROOT-MUSIC method [16]. θ_d can be modeled as $\theta_d = \widehat{\theta}_d + \Delta\theta_d$, where $\widehat{\theta}_d$ is the estimated angle from Alice to Bob, and $\Delta\theta_d$ represents the estimation error. $\Delta\theta_d$ is randomly distributed in a range of $[-\Delta\theta_{\max}, \Delta\theta_{\max}]$ such that the value of θ_d is randomly chosen. Let us denote α_n by the designed or ideal AB phase of antenna n at Alice. Considering the effect of QE, we establish the model of QE as follows

$$\widehat{\alpha}_n = \alpha_n + \Delta\alpha_n, \quad n \in 1, 2, \cdots, N_a, \tag{9}$$

where $\widehat{\alpha}_n \in \Theta$ is the quantized value of α_n after α_n passes through the corresponding phase quantizer. In the above model, the quantization error $\Delta\alpha_n$ is approximated as a uniform distribution and its probability density function (PDF) is given by

$$p(\Delta\alpha_n) = \begin{cases} \dfrac{1}{2\Delta\alpha_{\max}}, & \Delta\alpha_n \in [-\Delta\alpha_{\max}, \Delta\alpha_{\max}], \\ 0, & \text{otherwise}, \end{cases} \tag{10}$$

with

$$\Delta\alpha_{\max} = \frac{\pi}{2^L}, \tag{11}$$

where L is the number of quantization bits.

A. DERIVATION OF SINR LOSS DUE TO FINITE-BIT QUANTIZATION

Given the predesigned AB vector $\mathbf{v}_a(\alpha)$, we have

$$\begin{aligned} \mathbf{v}_a(\widehat{\alpha}) &= \frac{1}{\sqrt{N_a}}\left[e^{j\widehat{\alpha}_1}, e^{j\widehat{\alpha}_2}, \cdots, e^{j\widehat{\alpha}_{N_a}}\right]^T \\ &= \frac{1}{\sqrt{N_a}}\left[e^{j(\alpha_1+\Delta\alpha_1)}, e^{j(\alpha_2+\Delta\alpha_2)}, \cdots, e^{j(\alpha_{N_a}+\Delta\alpha_{N_a})}\right]^T. \end{aligned} \tag{12}$$

Substituting the above in (1), the RF transmit signal at Alice can be rewritten as

$$\mathbf{s}_a(\widehat{\alpha}) = \sqrt{P_a}\mathbf{v}_a(\widehat{\alpha})x. \tag{13}$$

In this case, the corresponding received signals at Bob and Eve can be respectively written as

$$\begin{aligned} y_b(\widehat{\alpha}) &= \sqrt{g_{ab}}\mathbf{h}_{ab}^H(\theta_d)\mathbf{s}_a(\widehat{\alpha}) + \sqrt{\rho}\mathbf{h}_{bb}^H\mathbf{s}_b + n_b \\ &= \sqrt{g_{ab}P_a}\mathbf{h}_{ab}^H(\theta_d)\mathbf{v}_a(\widehat{\alpha})x + \sqrt{\rho P_b}\mathbf{h}_{bb}^H\mathbf{v}_b z + n_b, \end{aligned} \tag{14}$$

and

$$\begin{aligned} y_e(\widehat{\alpha}) &= \sqrt{g_{ae}}\mathbf{h}_{ae}^H(\theta_e)\mathbf{s}_a(\widehat{\alpha}) + \sqrt{g_{be}}\mathbf{h}_{be}^H\mathbf{s}_b + n_e \\ &= \sqrt{g_{ae}P_a}\mathbf{h}_{ae}^H(\theta_e)\mathbf{v}_a(\widehat{\alpha})x + \sqrt{g_{be}P_b}\mathbf{h}_{be}^H\mathbf{v}_b z + n_e. \end{aligned} \tag{15}$$

Assuming that the ideal desired directional angle θ_d is available, we have

$$\alpha_n = 2\pi\Psi_{\theta_d}(n), \ \hat{\alpha}_n = 2\pi\Psi_{\theta_d}(n) + \Delta\alpha_n. \tag{16}$$

Substituting the above two equations in (14) and (15) yields

$$\begin{aligned} \mathbf{h}_{ab}^H(\theta_d)\mathbf{v}_a(\widehat{\alpha}) &= \left[e^{-j\alpha_1}, e^{-j\alpha_2}, \cdots, e^{-j\alpha_{N_a}}\right] \\ &\quad \times \frac{1}{\sqrt{N_a}}\left[e^{j(\alpha_1+\Delta\alpha_1)}, e^{j(\alpha_2+\Delta\alpha_2)}, \right. \\ &\quad \left. \cdots, e^{j(\alpha_{N_a}+\Delta\alpha_{N_a})}\right]^T \\ &= \frac{1}{\sqrt{N_a}}\sum_{n=1}^{N_a} e^{j\Delta\alpha_n}, \end{aligned} \tag{17}$$

and

$$\begin{aligned} \mathbf{h}_{ae}^H(\theta_e)\mathbf{v}_a(\widehat{\alpha}) &= \left[e^{-j\alpha_{ae,1}}, e^{-j\alpha_{ae,2}}, \cdots, e^{-j\alpha_{ae,N_a}}\right] \\ &\quad \times \frac{1}{\sqrt{N_a}}\left[e^{j(\alpha_1+\Delta\alpha_1)}, e^{j(\alpha_2+\Delta\alpha_2)}, \right. \\ &\quad \left. \cdots, e^{j(\alpha_{N_a}+\Delta\alpha_{N_a})}\right]^T \\ &= \frac{1}{\sqrt{N_a}}\sum_{n=1}^{N_a} e^{j(\alpha_n-\alpha_{ae,n}+\Delta\alpha_n)}, \end{aligned} \tag{18}$$

respectively. In (18), α_n is determined by (16), $\alpha_{ae,n}$ can be expressed similarly as (16) with known θ_e, $\alpha_{ae,n} = 2\pi\Psi_{\theta_e}(n)$.

In (17), $e^{j\Delta\alpha_i}(i = 1, 2, \cdots, N_a)$ can be viewed as independently identical distributed (iid) random variables, in accordance with the law of large numbers in probability theory. The mean of samples is approximately equal to the mean of the distribution [31]. As N_a tends to medium-scale and large-scale, we have

$$\frac{1}{N_a}\sum_{n=1}^{N_a} e^{j\Delta\alpha_n} \approx \mathbb{E}(e^{j\Delta\alpha_n}), \tag{19}$$

where

$$\begin{aligned}\mathbb{E}(e^{j\Delta\alpha_n}) &= \int_{-\Delta\alpha_{max}}^{\Delta\alpha_{max}} \mathrm{e}^{j\Delta\alpha_n} p(\Delta\alpha_n)\,\mathrm{d}\Delta\alpha_n \\ &= \frac{\sin(\Delta\alpha_{max})}{\Delta\alpha_{max}} \\ &= \mathrm{sinc}(\frac{\pi}{2^L}) \end{aligned} \tag{20}$$

with

$$\mathrm{sinc}(x) = \frac{\sin(x)}{x}. \tag{21}$$

Combining (19) and (20), one obtains

$$\frac{1}{N_a}\sum_{n=1}^{N_a} e^{j\Delta\alpha_n} \approx \mathrm{sinc}(\frac{\pi}{2^L}). \tag{22}$$

Now, we derive the expression of SINR at Bob under the QE and NQE conditions, respectively. The former has NQE while the latter has QE. From the definition of SINR and (14), we have

$$\mathrm{SINR}_b^{NQE} = \frac{g_{ab}P_a|\mathbf{h}_{ab}^H(\theta_d)\mathbf{v}_a(\alpha)|^2}{\rho P_b|\mathbf{h}_{bb}^H\mathbf{v}_b|^2+\sigma^2}, \tag{23}$$

$$\begin{aligned}\mathrm{SINR}_b^{QE} &= \frac{g_{ab}P_a|\mathbf{h}_{ab}^H(\theta_d)\mathbf{v}_a(\widehat{\alpha})|^2}{\rho P_b|\mathbf{h}_{bb}^H\mathbf{v}_b|^2+\sigma^2} \\ &= \frac{\mathbb{E}_{\widehat{\alpha}}\left[g_{ab}P_a|\mathbf{h}_{ab}^H(\theta_d)\mathbf{v}_a(\widehat{\alpha})|^2\right]}{\rho P_b|\mathbf{h}_{bb}^H\mathbf{v}_b|^2+\sigma^2} \\ &= \frac{g_{ab}P_aN_a\mathrm{sinc}^2(\frac{\pi}{2^L})}{\rho P_b|\mathbf{h}_{bb}^H\mathbf{v}_b|^2+\sigma^2}. \end{aligned} \tag{24}$$

According to (23) and (24), let us define the SINR performance loss γ as the ratio of SINR_b^{NQE} to SINR_b^{QE} at Bob as

$$\begin{aligned}\boldsymbol{\gamma} &= \frac{\mathrm{SINR}_b^{NQE}}{\mathrm{SINR}_b^{QE}} \\ &= \frac{1}{\mathrm{sinc}^2(\frac{\pi}{2^L})}. \end{aligned} \tag{25}$$

Observing the above expression and considering L is a positive integer, it is clear that increasing the value of L, i.e. the number of quantization bits, will reduce the SINR performance loss. In other words, the receive SINR performance will be improved gradually.

B. EXPRESSION OF SR WITH FINITE-BIT QUANTIZATION

In terms of (5) and (6), the achievable rates at Bob and Eve are as follows

$$R_b = \log_2\left(1+\frac{g_{ab}P_a|\mathbf{h}_{ab}^H\mathbf{v}_a|^2}{\rho P_b|\mathbf{h}_{bb}^H\mathbf{v}_b|^2+\sigma^2}\right), \tag{26}$$

and

$$R_e = \log_2\left(1+\frac{g_{ae}P_a|\mathbf{h}_{ae}^H\mathbf{v}_a|^2}{g_{be}P_b|\mathbf{h}_{be}^H\mathbf{v}_b|^2+\sigma^2}\right), \tag{27}$$

respectively, which yield the following achievable SR

$$\begin{aligned}R_s &= \max\{0, R_b - R_e\} \\ &= \max\left\{0, \log_2\left(\frac{MT+g_{ab}P_aT|\mathbf{h}_{ab}^H\mathbf{v}_a|^2}{MT+g_{ae}P_aM|\mathbf{h}_{ae}^H\mathbf{v}_a|^2}\right)\right\}, \end{aligned} \tag{28}$$

where

$$\begin{aligned}M &= \rho P_b|\mathbf{h}_{bb}^H\mathbf{v}_b|^2+\sigma^2, \\ T &= g_{be}P_b|\mathbf{h}_{be}^H\mathbf{v}_b|^2+\sigma^2. \end{aligned} \tag{29}$$

In the absence of QE, the corresponding SR is given by

$$\begin{aligned}R_s^{NQE} &= \max\left\{0, R_b^{NQE} - R_e^{NQE}\right\} \\ &= \max\left\{0, \log_2\left(\frac{MT+g_{ab}P_aT|\mathbf{h}_{ab}^H(\theta_d)\mathbf{v}_a(\alpha)|^2}{MT+g_{ae}P_aM|\mathbf{h}_{ae}^H(\theta_e)\mathbf{v}_a(\alpha)|^2}\right)\right\}. \end{aligned} \tag{30}$$

In terms of (18), we define

$$b_n \triangleq n - \frac{N_a+1}{2}, \tag{31}$$

$$q \triangleq -\frac{d}{\lambda}(\cos\theta_d - \cos\theta_e), \tag{32}$$

$$S_{N_a}(x) \triangleq \frac{\sin(N_a\pi x)}{\sin(\pi x)}. \tag{33}$$

Then, we rewrite (18) and define

$$\begin{aligned}\rho(b_n, \Delta\alpha_n) &\triangleq \mathbf{h}_{ae}^H(\theta_e)\mathbf{v}_a(\widehat{\alpha}) \\ &= \frac{1}{\sqrt{N_a}}\sum_{n=1}^{N_a} e^{j(\alpha_n-\alpha_{ae,n}+\Delta\alpha_n)} \\ &= \frac{1}{\sqrt{N_a}}\sum_{n=1}^{N_a} e^{j(2\pi qb_n+\Delta\alpha_n)}. \end{aligned} \tag{34}$$

The mean of $|\mathbf{h}_{ae}^H(\theta_e)\mathbf{v}_a(\widehat{\alpha})|^2$, or $|\rho(b_n, \Delta\alpha_n)|^2$ is derived as

$$\begin{aligned}&\mathbb{E}_{\widehat{\alpha}}[|\mathbf{h}_{ae}^H(\theta_e)\mathbf{v}_a(\widehat{\alpha})|^2] \\ &= \mathbb{E}_{\Delta\alpha_n}[\rho^*(b_n, \Delta\alpha_n)\rho(b_n, \Delta\alpha_n)] \\ &= \frac{1}{N_a}\mathbb{E}_{\Delta\alpha_n,\Delta\alpha_{n'}}\left\{\sum_{n=1}^{N_a}\sum_{n'=1}^{N_a} e^{-j(2\pi qb_n+\Delta\alpha_n)}e^{j(2\pi qb_{n'}+\Delta\alpha_{n'})}\right\} \\ &= \frac{1}{N_a}\mathbb{E}_{\Delta\alpha_n}\left\{\sum_{n=1}^{N_a} e^{-j(2\pi qb_n+\Delta\alpha_n)}e^{j(2\pi qb_n+\Delta\alpha_n)}\right\} + \frac{1}{N_a} \\ &\quad\cdot\mathbb{E}_{\Delta\alpha_n,\Delta\alpha_{n'}}\left\{\sum_{n=1,n\neq n'}^{N_a}\sum_{n'=1}^{N_a} e^{-j(2\pi qb_n+\Delta\alpha_n)}e^{j(2\pi qb_{n'}+\Delta\alpha_{n'})}\right\} \\ &= \frac{N_a}{N_a} + \frac{1}{N_a}\left\{\int_{-\Delta\alpha_{max}}^{\Delta\alpha_{max}} e^{j\Delta\alpha_n}p(\Delta\alpha_n)\,\mathrm{d}\Delta\alpha_n\int_{-\Delta\alpha_{max}}^{\Delta\alpha_{max}} e^{j\Delta\alpha_{n'}}\right. \\ &\quad\left.\cdot\,p(\Delta\alpha_{n'})\,\mathrm{d}\Delta\alpha_{n'}\right\}\left\{\sum_{n=1,n\neq n'}^{N_a}\sum_{n'=1}^{N_a} e^{-j2\pi qb_n}e^{j2\pi qb_{n'}}\right\} \\ &= 1 + \frac{1}{N_a}\mathrm{sinc}^2(\frac{\pi}{2^L})\left(S_{N_a}^2(q) - N_a\right), \end{aligned} \tag{35}$$

and the corresponding SR is given by

$$
\begin{aligned}
&R_s^{QE} \\
&= \max\left\{0, R_b^{QE} - R_e^{QE}\right\} \\
&= \max\left\{0, \log_2\left(\frac{MT + g_{ab}P_aT|\mathbf{h}_{ab}^H(\theta_d)\mathbf{v}_a(\widehat{\alpha})|^2}{MT + g_{ae}P_aM|\mathbf{h}_{ae}^H(\theta_e)\mathbf{v}_a(\widehat{\alpha})|^2}\right)\right\} \\
&= \max\left\{0, \log_2\left(\frac{\mathbb{E}_{\widehat{\alpha}}\left[MT + g_{ab}P_aT|\mathbf{h}_{ab}^H(\theta_d)\mathbf{v}_a(\widehat{\alpha})|^2\right]}{\mathbb{E}_{\widehat{\alpha}}\left[MT + g_{ae}P_aM|\mathbf{h}_{ae}^H(\theta_e)\mathbf{v}_a(\widehat{\alpha})|^2\right]}\right)\right\} \\
&= \max\left\{0, \log_2\left(\frac{MT + g_{ab}P_aTN_a\mathrm{sinc}^2(\frac{\pi}{2^L})}{MT + g_{ae}P_aM\mathbb{E}_{\widehat{\alpha}}\left[|\mathbf{h}_{ae}^H(\theta_e)\mathbf{v}_a(\widehat{\alpha})|^2\right]}\right)\right\} \\
&= \max\Bigg\{0, \\
&\quad \log_2\left(\frac{MT + g_{ab}P_aTN_a\mathrm{sinc}^2(\frac{\pi}{2^L})}{MT + g_{ae}P_aM(1 - \mathrm{sinc}^2(\frac{\pi}{2^L}) + \frac{\mathrm{sinc}^2(\frac{\pi}{2^L})S_{N_a}^2(q)}{N_a})}\right)\Bigg\}.
\end{aligned}
\tag{36}
$$

IV. SIMULATION AND DISCUSSION

In this section, we mainly focus on the evaluation of impact of the number of antennas and quantization bits of phase shifters on performance losses including bit error rate (BER), SINR and SR in an AB structure. In the simulation, system parameters are chosen as follows: quadrature phase shift keying (QPSK) modulation, the total transmission power $P_a = P_b = 70$ dBm, the spacing between two adjacent antennas $d = \lambda/2$, $\rho = 0.5$, the distance between Alice and Bob, Alice and Eve, Bob and Eve $d_{ab} = d_{ae} = d_{be} = 500$ m, the path loss exponent $c = 2$, the desired direction $\theta_d = \theta_{ab} = 60°$, and the eavesdropping direction $\theta_e = \theta_{ae} = 120°$. The direction angle from Bob to Eve is $\theta_{be} = 45°$. Alice is equipped with N_a antennas, Bob is equipped with $N_b^t = 16$ antennas to transmit AN and $N_b^r = 1$ to receive confidential signals from Alice.

Fig. 2 demonstrates the performance curves of BER versus direction angle at Bob with SNR $= 10$ dB and $N_a = 16$. Here, the ideal condition implies NQE with solid line, i.e., infinite bits for quantization, and the QE case is denoted by dotted line. L stands for the number of quantization bits. From this figure, it can be seen that the BER can achieve a good performance in the desired direction while it becomes worse rapidly as we move to the undesired direction. This is partly because the AN transmitted from Bob can interfere with the confidential signal received at Eve severely along the undesired directions. Compared with the performance with NQE, the BER performance with QE is much worse, especially for $L \leq 2$. As L reaches up to 3, the BER performance difference between QE and NQE is trivial. This means that it is feasible in practice to use finite-quantized phase shifters with $L = 3$.

Fig. 3 plots the curves of SINR performance loss versus number L of quantization bits ranging from 1 to 8 for four different numbers of antennas at Alice N_a: 4, 16, 64, and 256, where SNR is equal to 15 dB. Here, the derived expression of SINR performance loss in (25) is used as a performance reference. From this figure, it is seen that the

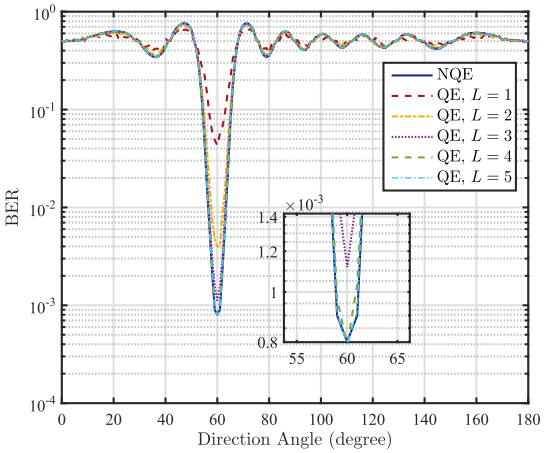

FIGURE 2. Curves of BER versus direction angle under the ideal condition (with NQE) and finite-quantization condition (with QE) for different numbers (L) of quantization bits.

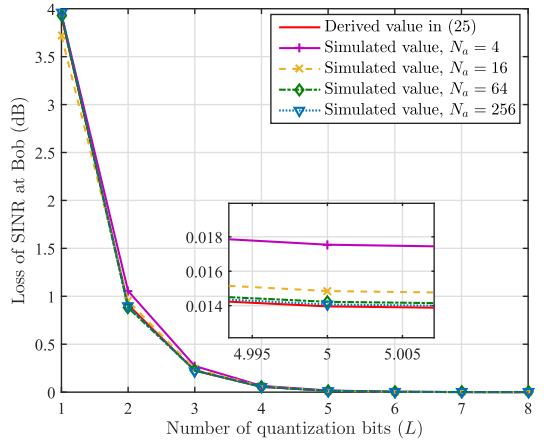

FIGURE 3. SINR performance loss at Bob versus number L of quantization bits for different N_a.

performance loss of simulated SINR decreases as the quantization bits increases. This is mainly because that the range of phase error due to quantization (11) will become smaller as the number L of quantization bits increases, so that QE will become smaller. This will result in a smaller loss of SINR at Bob. A small number of quantization bits of the phase shifter (e.g., $L = 1$ or 2) will cause a large QE, resulting in a large SINR loss up to 4 dB. The SINR performance loss will be less than 0.3 dB when the number of quantization bits is more than or equal to 3. When the number of quantization bits is 4, the SINR loss at Bob is less than 0.1 dB even if the number of antennas at Alice is small (e.g., $N_a = 3$). This also means the fact that even with a small number of antennas at Alice, the derived expression in (25) coincides with the simulated SINR performance loss. In other words, the derived expression in (25) can be used to evaluate the SINR performance loss for almost all cases including small-scale, medium-scale, and large-scale. More importantly, we can conclude that three quantization bits are sufficient for the quantized phase shifters in the AB system.

Since we have the approximate derived simple expression for SINR performance loss, Fig. 4 illustrates the curves of the

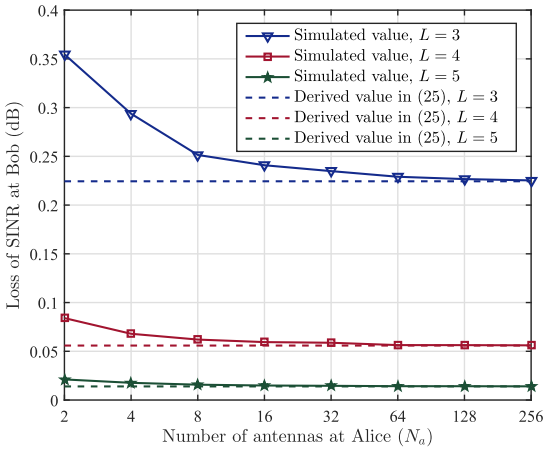

FIGURE 4. SINR performance loss at Bob versus N_a for different numbers of quantization bits (L).

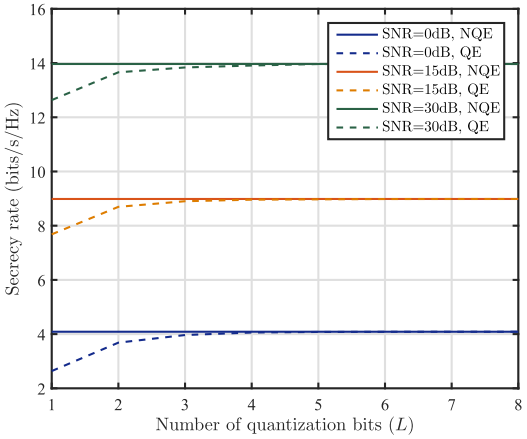

FIGURE 5. Secrecy rate versus number L of quantization bits for different transmit SNR in two cases NQE and QE with $N_a = 16$.

SINR performance loss versus the number N_a of antennas at Alice for three different numbers of quantization bits: 3, 4, and 5, where the SNR is set to be 15 dB. From this figure, it is seen that the simulated value of SINR loss gradually tends to the derived value in (25) as the number of antennas at Alice increases. Even in the case of small number of antennas at Alice, the SINR loss difference between simulated and derived is still only about 0.125 dB, which is substantially small. This further verifies the validity of the derived expression in (25).

Fig. 5 shows the curves of SR versus number of quantization bits ranging from 1 to 8 for three typical SNRs: 0 dB, 15 dB, and 30 dB, where $N_a = 16$. The solid lines represent the SR in the absence of QE, and the dotted lines represent the approximate derived value of SR in the presence of QE in (36) for different SNR. From this figure, it is clearly seen that there is a certain loss on SR for the small number of quantization bits, i.e., $L = 1$ or 2. Observing this figure, a 3-quantization-bit phase shifters at Alice will lead to a SR performance loss less than 0.1 bits/s/Hz.

Fig. 6 shows the curves of SR versus number of quantization bits for four different numbers of antennas at Alice N_a: 4, 16, 64, and 256 with three typical SNRs: 0 dB, 15 dB,

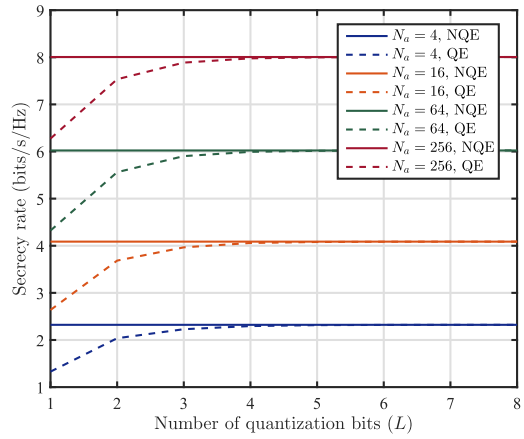

(a) SNR = 0 dB

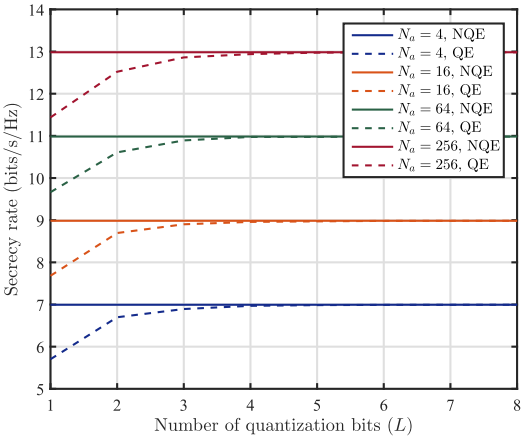

(b) SNR = 15 dB

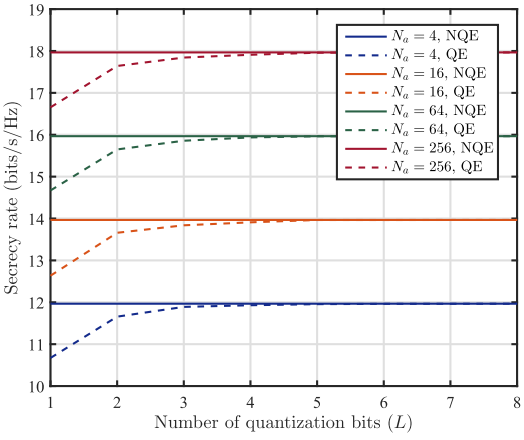

(c) SNR = 30 dB

FIGURE 6. Secrecy rate versus number L of quantization bits for different N_a and different transmit SNR in two cases NQE and QE.

and 30 dB. The solid lines represent the SR in the absence of QE, and the dotted lines represent the approximate derived value of SR in the presence of QE in (36) for different N_a. It can be seen from the figure that three-quantization-bit achieves a SR performance loss of less than 0.1 bits/s/Hz regardless of the number of transmit antennas at Alice. The range of the quantized phases in (4) is determined by the number of quantization bits L. The larger the quantization

bits L, the more the selectable phases of the quantized phases are in (4). When L is sufficiently small (e.g., $L = 1, 2$), the number of selectable value corresponding to the quantized phases in (4) is small. This means that the error between the quantized phase corresponding to each antenna in the analog beamforming vector and the ideal designed phase is large. In this case, R_s^{QE} is much smaller than R_s^{NQE}, which can be seen in Fig. 5 and Fig. 6. When L approaches infinity, we can see R_s^{QE} precisely matches R_s^{NQE}, which can be examined in (36).

In summary, there exists QE in the AB structure due to finite-quantized phase shifters, which will result in a substantial performance loss. In general, from the above simulation results and derived SINR performance loss expression as shown in (25), we find an important fact that 3, 4, and 5 are sufficient for the number of quantization bits on RF phase shifter such that a performance loss due to QE can be neglected. The derived simple expression in (25) can be approximately used to assess the SINR performance loss at Bob. Additionally, this expression also holds for even small number of transmit antennas at Alice although it is derived under the condition that the number of antennas at Alice tends to large-scale. This expression can be directly applied in the HAD structure to evaluate the SINR loss.

V. CONCLUSION

In this paper, we have made an investigation of the impact of QE caused by finite-quantized phase shifters of AB structure on performance in DM systems. In the presence of QE, the expression of SINR performance loss has been derived to be inversely proportional to the square of sinc function by making use of the law of large numbers in probability theory. From analysis and simulation, we have found that our proposed expression is approximately close to the corresponding simulated result even when the number of antennas at Alice is small-scale. The SINR performance loss is lower than 0.3 dB when the number of quantization bits is larger than or equal to 3. As for SR, we can obtain the same result. In other words, when the number of quantization bits is larger than or equal to 3, the SR difference between NQE and QE is less than 0.1 bits/s/Hz. Additionally, the BER performance is also shown to be intimately related to the number of quantization bits. A large L means a good BER performance along the desired direction. Otherwise, a small L means a poor BER performance along the desired direction. Considering the derived SINR performance loss holds for small-scale number of antennas at Alice in AB structure, it is sensible to extend it to a HAD beamforming structure with finite-quantized phase shifters in diverse scenarios for future wireless communications.

REFERENCES

[1] M. P. Daly and J. T. Bernhard, "Directional modulation technique for phased arrays," *IEEE Trans. Antennas Propag.*, vol. 57, no. 9, pp. 2633–2640, Sep. 2009.
[2] M. P. Daly and J. T. Bernhard, "Beamsteering in pattern reconfigurable arrays using directional modulation," *IEEE Trans. Antennas Propag.*, vol. 58, no. 7, pp. 2259–2265, Jul. 2010.
[3] H. Shi and A. Tennant, "Secure physical-layer communication based on directly modulated antenna arrays," in *Proc. Loughborough Antennas Propag. Conf. (LAPC)*, Loughborough, U.K., Nov. 2012, pp. 1–4.
[4] Y. Ding and V. F. Fusco, "A vector approach for the analysis and synthesis of directional modulation transmitters," *IEEE Trans. Antennas Propag.*, vol. 62, no. 1, pp. 361–370, Jan. 2014.
[5] S. Yan, N. Yang, I. Land, R. Malaney, and J. Yuan, "Three artificial-noise-aided secure transmission schemes in wiretap channels," *IEEE Trans. Veh. Technol.*, vol. 67, no. 4, pp. 3669–3673, Apr. 2018.
[6] S. Yan, Y. Cong, S. V. Hanly, and X. Zhou, "Gaussian signalling for covert communications," *IEEE Trans. Wireless Commun.*, vol. 18, no. 7, pp. 3542–3553, Jul. 2019.
[7] F. Shu, T. Xu, J. Hu, and S. Yan, "Delay-constrained covert communications with a full-duplex receiver," *IEEE Wireless Commun. Lett.*, vol. 8, no. 3, pp. 813–816, Jun. 2019.
[8] J. Hu, S. Yan, F. Shu, J. Wang, J. Li, and Y. Zhang, "Artificial-noise-aided secure transmission with directional modulation based on random frequency diverse arrays," *IEEE Access*, vol. 5, pp. 1658–1667, 2017.
[9] J. S. Hu, F. Shu, and J. Li, "Robust synthesis method for secure directional modulation with imperfect direction angle," *IEEE Commun. Lett.*, vol. 20, no. 6, pp. 1084–1087, Jun. 2016.
[10] F. Shu, X. Wu, J. Li, R. Chen, and B. Vucetic, "Robust synthesis scheme for secure multi-beam directional modulation in broadcasting systems," *IEEE Access*, vol. 4, pp. 6614–6623, 2016.
[11] F. Shu, W. Zhu, X. Zhou, J. Li, and J. Lu, "Robust secure transmission of using main-lobe-integration-based leakage beamforming in directional modulation MU-MIMO systems," *IEEE Systems J.*, vol. 12, no. 4, pp. 3775–3785, Dec. 2018.
[12] F. Shu, L. Xu, J. Wang, W. Zhu, and Z. Xiaobo, "Artificial-noise-aided secure multicast precoding for directional modulation systems," *IEEE Trans. Veh. Technol.*, vol. 67, no. 7, pp. 6658–6662, Jul. 2018.
[13] H. Zhu and J. Wang, "Chunk-based resource allocation in OFDMA systems—Part I: Chunk allocation," *IEEE Trans. Commun.*, vol. 57, no. 9, pp. 2734–2744, Sep. 2009.
[14] H. Zhu and J. Wang, "Chunk-based resource allocation in OFDMA systems—Part II: Joint chunk, power and bit allocation," *IEEE Trans. Commun.*, vol. 60, no. 2, pp. 499–509, Feb. 2012.
[15] F. Shu, X. Wu, J. Hu, J. Li, R. Chen, and J. Wang, "Secure and precise wireless transmission for random-subcarrier-selection-based directional modulation transmit antenna array," *IEEE J. Sel. Areas Commun.*, vol. 36, no. 4, pp. 890–904, Apr. 2018.
[16] F. Shu, Y. Qin, T. Liu, L. Gui, Y. Zhang, J. Li, and Z. Han, "Low-complexity and high-resolution DOA estimation for hybrid analog and digital massive MIMO receive array," *IEEE Trans. Commun.*, vol. 66, no. 6, pp. 2487–2501, Jun. 2018.
[17] O. El Ayach, S. Rajagopal, S. Abu-Surra, Z. Pi, and R. W. Heath, Jr., "Spatially sparse precoding in millimeter wave MIMO systems," *IEEE Trans. Wireless Commun.*, vol. 13, no. 3, pp. 1499–1513, Mar. 2014.
[18] A. Alkhateeb, O. El Ayach, G. Leus, and R. W. Heath, Jr., "Channel estimation and hybrid precoding for millimeter wave cellular systems," *IEEE J. Sel. Topics Signal Process.*, vol. 8, no. 5, pp. 831–846, Oct. 2014.
[19] Y.-Y. Lee, C.-H. Wang, and Y.-H. Huang, "A hybrid RF/baseband precoding processor based on parallel-index-selection matrix-inversion-bypass simultaneous orthogonal matching pursuit for millimeter wave MIMO systems," *IEEE Trans. Signal Process.*, vol. 63, no. 2, pp. 305–317, Jan. 2015.
[20] J. Wang, Z. Lan, C.-W. Pyo, T. Baykas, C.-S. Sum, M. A. Rahman, R. Funada, F. Kojima, I. Lakkis, H. Harada, and S. Kato, "Beam codebook based beamforming protocol for multi-Gbps millimeter-wave WPAN systems," *IEEE J. Sel. Areas Commun.*, vol. 27, no. 8, pp. 1390–1399, Oct. 2009.
[21] V. Venkateswaran and A. van der Veen, "Analog beamforming in MIMO communications with phase shift networks and online channel estimation," *IEEE Trans. Signal Process.*, vol. 58, no. 8, pp. 4131–4143, Aug. 2010.
[22] Y. M. Tsang, A. S. Y. Poon, and S. Addepalli, "Coding the beams: Improving beamforming training in mmwave communication system," in *Proc. IEEE Global Telecommun. Conf. (GLOBECOM)*, Houston, TX, USA, Dec. 2011, pp. 1–6.
[23] S. Hur, T. Kim, D. J. Love, J. V. Krogmeier, T. A. Thomas, and A. Ghosh, "Millimeter wave beamforming for wireless backhaul and access in small cell networks," *IEEE Trans. Commun.*, vol. 61, no. 10, pp. 4391–4403, Oct. 2013.
[24] W. C. Jakes, *Microwave Mobile Communications*. New York, NY, USA: Wiley, 1974.

[25] S. Yan, N. Yang, R. Malaney, and J. Yuan, "Antenna switching for security enhancement in full-duplex wiretap channels," in *Proc. IEEE Globecom Workshops*, Dec. 2014, pp. 1308–1313.
[26] G. Zheng, I. Krikidis, J. Li, A. P. Petropulu, and B. Ottersten, "Improving physical layer secrecy using full-duplex jamming receivers," *IEEE Trans. Signal Process.*, vol. 61, no. 20, pp. 4962–4974, Oct. 2013.
[27] S. Yan, N. Yang, G. Geraci, R. Malaney, and J. Yuan, "Optimization of code rates in SISOME wiretap channels," *IEEE Trans. Wireless Commun.*, vol. 14, no. 11, pp. 6377–6388, Nov. 2015.
[28] H. Yu, S. Wan, W. Cai, L. Xu, X. Zhou, J. Wang, Y. Wu, F. Shu, J. Wang, and J. Wang, "GPI-based secrecy rate maximization beamforming scheme for wireless transmission with AN-aided directional modulation," *IEEE Access*, vol. 6, pp. 12044–12051, 2018.
[29] N. Lee, H. J. Yang, and J. Chun, "Achievable sum-rate maximizing AF relay beamforming scheme in two-way relay channels," in *Proc. IEEE Int. Conf. Commun. Workshops (ICC Workshops)*, May 2008, pp. 300–305.
[30] S. Yan, X. Zhou, N. Yang, T. D. Abhayapala, and A. L. Swindlehurst, "Secret channel training to enhance physical layer security with a full-duplex receiver," *IEEE Trans. Inf. Forensics Security*, vol. 13, no. 11, pp. 2788–2800, Nov. 2018.
[31] L. Wasserman, *All of Statistics: A Concise Course in Statistical Inference*. New York, NY, USA: Springer, 2004.

JIAYU LI received the B.S. degree from the Nanjing University of Science and Technology, China, in 2018, where she is currently pursuing the M.S. degree with the School of Electronic and Optical Engineering. Her research interests include wireless communication, signal processing, and mobile networks.

LING XU received the B.S. degree from the Nanjing University of Science and Technology, China, in 2017, where she is currently pursuing the M.S. degree with the School of Electronic and Optical Engineering. Her research interests include wireless communications and mobile networks.

PING LU received the Doctor of Engineering (D.Eng.) degree in electronic and information engineering from South East University. He is currently the President of the Cloud Computing and Enterprise Service Product of ZTE Corporation. His research interests include cloud computing, big data, augmented reality, and multimedia services-based techniques.

TINGTING LIU (M'12) received the B.S. degree in communication engineering and the Ph.D. degree in information and communication engineering from the Nanjing University of Science and Technology, Nanjing, China, in 2005 and 2011, respectively. Since 2011, she has been with the School of Communication Engineering, Nanjing Institute of Technology, China. She is currently a Postdoctoral with the Nanjing University of Science and Technology. Her research interests include vehicular fog computing, QoS, game theory, caching-enabled systems, device-to-device networks, and cognitive radio networks.

ZHIHONG ZHUANG is currently a Professor with the School of Electronic and Optical Engineering, Nanjing University of Science and Technology, China. His research interests include signal analysis technology, short-range detecting, and underwater target detection technology.

JINSONG HU received the B.S. and Ph.D. degrees from the School of Electronic and Optical Engineering, Nanjing University of Science and Technology, Nanjing, China, in 2013 and 2018, respectively. From 2017 to 2018, he was a Visiting Ph.D. Student with the Research School of Engineering, The Australian National University, Canberra, ACT, Australia. He is currently a Lecturer with the College of Physics and Information Engineering, Fuzhou University, Fuzhou, China. He served as a TPC member for the IEEE ICC 2019 and IEEE GLOBECOM 2019. His research interests include array signal processing, covert communications, and physical layer security.

FENG SHU (M'16) was born in 1973. He received the B.S. degree from the Fuyang Teaching College, Fuyang, China, in 1994, the M.S. degree from Xidian University, Xi'an, China, in 1997, and the Ph.D. degree from Southeast University, Nanjing, China, in 2002. In 2005, he joined the School of Electronic and Optical Engineering, Nanjing University of Science and Technology, Nanjing, where he is currently a Professor, and also a Supervisor of the Ph.D. degree and graduate students. From 2009 to 2010, he held a visiting postdoctoral position with The University of Texas at Dallas. He has published about 300 papers, of which over 200 are in archival journals, including more than 60 papers on the IEEE Journals and more than 100 SCI-indexed papers. He holds seven Chinese patents. His research interests include wireless networks, wireless location, and array signal processing. He serves as a TPC member for several international conferences, including the IEEE ICC 2019, the IEEE ICCS 2018/2016, ISAPE 2018, and WCSP 2017/2016/2014. He was the Mingjiang Chair Professor in Fujian Province. He is currently an Editor of the journal IEEE Access.

JIANGZHOU WANG (F'17) is currently a Professor and the former Head of the School of Engineering and Digital Arts, University of Kent, U.K. He has published over 300 papers in international journals and conferences and four books in the areas of wireless mobile communications.

Prof. Wang is also a Fellow of the Royal Academy of Engineering, U.K. He received the Best Paper Award from the IEEE GLOBECOM2012. He was the IEEE Distinguished Lecturer, from 2013 to 2014. He was the Technical Program Chair of the IEEE WCNC 2013 and the IEEE International Conference on Communications (ICC 2019), Shanghai. He was also the Executive Chair of the IEEE ICC 2015, London. He has served as an Editor for a number of international journals, including the IEEE Transactions on Communications, from 1998 to 2013.